Platform image processing to study the structural properties of retinal vessel

Gabino Verde[a], Luis García-Ortiz[b], Carolina Zato[a], Juan F. De Paz[a], Sara Rodríguez[a] and Miguel A. Merchán[b]

[a] Computers and Automation Department, University of Salamanca, Salamanca, Spain

[b] Primary care Research unit La Alamedilla. Sacyl. IBSAL. Salamanca. Spain.

KEYWORD

arterial stiffness;
cardiovascular disease;
AI algorithms;
pattern recognition,
image analysis;

ABSTRACT

This paper presents a technological platform specialized in assessing retinal vessel caliber and describing the relationship of the results obtained to cardiovascular risk. Retinal circulation is an area of active research by numerous groups, and there is general experimental agreement on the analysis of the patterns of the retinal blood vessels in the normal human retina. The development of automated tools designed to improve performance and decrease interobserver variability, therefore, appears necessary.

1 Introduction

The vascular system in the human retina is easily observed in its natural living state in the human retina by the use of a retinal camera. The retina is the only human location where blood vessels can be directly visualized non-invasively. The identification of landmark features such as the optic disc, fovea and the retinal vessels as reference co-ordinates is a prerequisite to systems being able to achieve more complex tasks that identify pathological entities. Reliable techniques exist for identifying these structures in retinal photographs. The most studied areas in this field can be classified into three groups [17]: (i) The detection of the fovea, usually chosen as the position of maximum correlation between a model template and the intensity image [15]. (ii) The location of the optic disc, which is important in retinal image analysis for vessel tracking, as a reference length for measuring distances in retinal images, and for identifying changes within the optic disc region due to disease. Techniques such as analysis of intensity pixels with a high grey-scale value [14][6] or principal component analysis (PCA) [15] are used for locating the disk. Other authors [13] use the Hough transform (a general technique for identifying the locations and orientations of certain types of shapes within a digital image [13]) to locate the optic disc. A ‘‘fuzzy convergence’’ algorithm is another technique used for this goal [7]. (iii) The segmentation of the vasculature form retinal images, that is, the representation of the blood vessels and their connections by segments or similar structures [2] [10] [16] [11] [7].

In this work is proposed a novel platform image processing to study the structural properties of vessels, arteries and veins that are observed with a red-free fundus camera in the normal human eye, and the fractal analysis of the branching trees of the vascular system. The platform, called Altair "Automatic image analyzer to assess retinal vessel caliber", employs analytical methods and AI (Artificial Intelligence) algorithms to detect retinal parameters of interest. The sequence of algorithms represents a new methodology to determine the properties of retinal veins and arteries. The platform uses the latest computer techniques both statistical and medical.

The next section presents the platform. Section 2 presents the most important characteristics of the platform, showing some of the relevant techniques and results. Finally, some conclusions and future work are presented in section 3.

2 Platform image processing

The platform facilitates the study of structural properties of vessels, arteries and veins that are observed with a red-free fundus camera in the normal human eye, and the fractal analysis of the branching trees of the vascular system. The main goal is to relate the level of cardiovascular risk in patients to everything that can be observed in the retinas. In this work we are interested in obtaining as much information as possible from the images obtained (Index Artery / Vein, Branching, Area occupied by the veins and arteries, Distribution of the capillary). Figure 1 shows an example of images taken directly from the fundus. The retinal vessels appear in a different color, with the optic disc and fovea.

Fig. 1. Retinograph image

The original image passes through each one of the modules (preprocessing, detection, segmentation and extraction of knowledge), which use different techniques and algorithms to obtain the desired image information.

Firstly, a phase called "digitization of the retina", in which the different parts of the eye image are identified. Here a data structure is created, which makes it possible to represent and process the retina without requiring the original image. This phase includes steps of preprocessing, detection and segmentation. Secondly, a phase of "measurements" in which we work with retinas that have been previously identified. This phase includes extraction of knowledge and manual correction, or expert knowledge, if necessary.

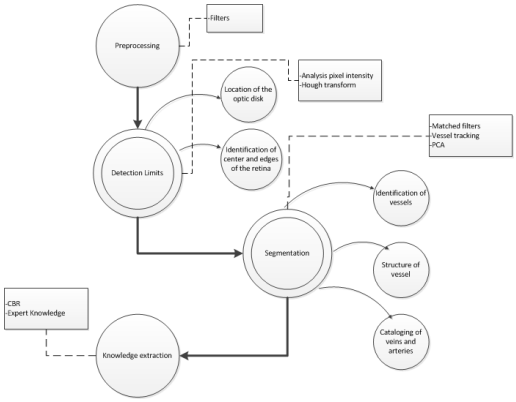

Fig. 2: Outline of the platform

The *preprocessing* step reduces noise, improves contrast, sharpens edges or corrects blurriness. Some of these actions can be carried out at the hardware level, which is to say with the features included with the camera. During the testing, retinography was performed using a Topcon TRC NW 200 nonmydriatic retinal camera (Topcon Europe B.C., Capelle a/d Ijssel, The Netherlands), obtaining nasal and temporal images centered on the disk (Figure 1). The nasal image with the centered disk is loaded into the platform software through the preprocessing module.

The *identification of the papilla* is important since it serves as the starting point for the detection and identification of the different blood vessels. This phase identifies the boundaries and the retinal papilla from a RGB image of the retina. The following values are returned: Cr is the center of the retina, which identifies the vector with coordinates x, y of the center of the retina. Cp is the center of the disc, which identifies the vector with the coordinates x, y of the center of the papilla. Rr, is the radius of the retina. Rp, is the radius of the papilla.

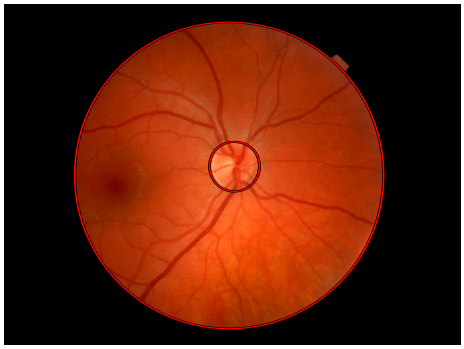

Fig. 3: Identification result in the detection phase.

C_r	C_p	R_r	R_p
1012,44 ; 774,13	**1035,98 ; 734,11** 1104,87 ; 562,52 915,38 ; 736,77 900,27 ; 658,74	**692,68**	**111,76** 108,92 122,15 101,95

Table 1. Sequence of output values in detection modules (pixel)

To carry out the identification of the limits, and in particular to the identification of the circumferences, it became necessary to carry out a process of image segmentation. Segmentation is the process that divides an image into regions or objects whose pixels have similar attributes. Each segmented region typically has a physical significance within the image. It is one of the most important processes in an automated vision system because allows to extract the objects from the image for subsequent description and recognition. Segmentation techniques can be grouped in three main groups: techniques based on the detection of edges or borders **¡Error! No se encuentra el origen de la referencia.**, thresholding techniques **¡Error! No se encuentra el origen de la referencia.** and techniques based on clustering of pixels **¡Error! No se encuentra el origen de la referencia.**. After analyzing the possibilities we chose one of the techniques of the first group that provided the best results. In this case using an optimization of the Hough transform **¡Error! No se encuentra el origen de la referencia.**. This technique is very robust against noise and the existence of gaps in the border of the object. It is used to detect different shapes in digital images. When applying the Hough transform to an image must first obtain a binary image of the pixels that form part of the limits of the object (applying edge detection). The aim of the Hough transform is found aligned points that may exist in the image to form a desired shape. For example, to identify a line points that satisfy the equation of the line: ($\varrho = x \cdot cos\ \theta + sen\ \theta$, in polar coordinate). In our case, we look for points that verify the equation of the circle:

- In polar coordinate system: $r^2 - 2sr \cdot cos(\theta - \alpha) + s^2 = c^2$, where (s, α) is the center and c the radius.
- In cartesian coordinate system: $(x-a)^2 + (y-b)^2=r^2$, where (a,b) is the center and r the radius.

For the algorithm is not computationally heavy, does not check all radios, or all possible centers, only the candidate values. The candidates centers are those defined in a near portion of the retina and the radius are in approximately one sixth the radius of the retina. To measure the approximate diameter of the retina, the algorithm calculates the average color of the image column: diameter of the retina is the length that has non-zero value (black).

Having identified the papilla (Figure 3) is a necessary step because it provides a starting point for other stages of segmentation and reference point for some typical measurements. Typically the correct result is the circumference of the higher value in the accumulator (over 70% of cases). In almost 100% of the cases, the correct identification is between the first 3 greatest accumulator values having.

The ultimate s in this step is to identify each blood vessel as a series of points that define the path of the vessel. Each of these points will be assigned a certain thickness. Moreover, it will be necessary to distinguish whether a particular blood vessel is a vein or an artery. AI algorithms responsible for identifying veins and arteries must perform a series of sweeps in search of "key points". Algorithms based on matched filters[2] [10] [16] [11], vessel tracking [19] and PCA [15], among others, are used for obtaining the proximity points between objects (veins, arteries, capillaries), the structures retinal structures or assemblies, branching patterns, etc. These algorithms work with transformations of the original image of the retina obtained from the previous step. Three steps are necessary within this module: (i) identification of vessels; (ii) definition of the structure of vessel; (iii) cataloging of veins and arteries.

2.1 Vessel identification

In this step the blood vessels are identified in the image by thresholding techniques. Its purpose is to remove pixels where no enters the structuring element, in this case the blood vessels. The image on the retina is blurred to keep an image similar to the background. This image is used as a threshold so that the pixels of the original image will be treated as vessels if its intensity reaches 90% of the background intensity. The image below represents the application of the-

se techniques in a row. The blue line represents the values of the pixels in the image; the red line, the background values; and the green line the point where there is a vessel:

Fig. 4. Thresholding techniques for the identification of vessels

In the figure it is possible to observe that on the left there is a very small vessel artery from below. In the middle is a fat vein and right three tiny vessels. Furthermore the edge of the retina is marked as a vessel although obviously not is. To decide where there is a vessel and where, it applies the following algorithm (Figure 7a). Where Original(x,y) is the pixel (x,y) of the original image and Background(x,y) is the pixel (x,y) of the background image.

2.2 Vessel Structure

This phase defines the tree forming blood vessels. Various techniques are used in conjunction with the following steps:

Step 1: Identification of connected components

- Dilate the binary image of the vessels (horizontally and vertically) to join possible discontinuities.
- Identify the connected component of the papilla. The remainder are discarded, will mostly noise points. Labeling.

Step 2: Morphological image processing.

- Choose corona of 10 pixels thick around the disc.
- Search regions in the corona. The center of gravity of each region found is taken as the starting point of a vessel.
- Choose another corona of 10 pixels around the former so that they overlap slightly.
- Search regions in the new corona. The center of gravity of each region corresponds to a found point of a vessel skeleton. If a region of this corona shares some pixel with the previous corona, join both points (nodes) with an edge.
- Repeat the above two points to cover the entire surface of the retina.

```
Step 3: Resolution of conflicts such as
vessel bifurcations or crossovers.
```

Fig. 5: Pseudocode of the identification algorithm of the structure of the vessels

The following image shows the output of this phase. At the end of this stage the whole arterio-venous tree is stored in a structured way that not only allows to know if a vessel passes for a point or not, but it also is known through which passes each vessel, which is its parent, etc.

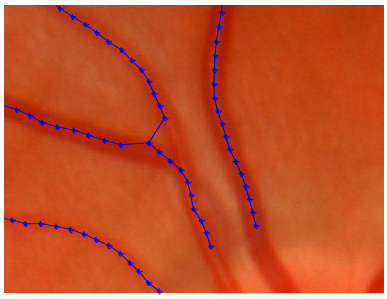

Fig. 6: Structure of the vessels

2.2 Veins and arteries catalogue

To detect whether a vessel is vein or artery, main branch is taken of the vessel. For every point (x, y) of the branch:

```
If (Original (x,y) < Background (x,y) *
threshold)
     Probable vein
If not
     Not vein
Threshold ~0.7
```

Figure 10: a) Pseudocode of the identification algorithm of veins.

In general, if most of the points of the main branch of the vessel (from 60%) are points classified as "probable vein", we conclude that this vessel is a vein, otherwise an artery. Currently, there are no publicly available databases that can be used to assess the performance of automatic detection algorithms on retinal images. In this work, we assessed the performance of our platform using retinal images acquired from Primary Care Research Unit La Alamedilla, SACYL, IBSAL, Salamanca, Spain . The images were obtained using a TopCon TRC-NW6S Non-Mydriatic Retinal Camera. Figure 7 show the testing performed using 10 retinal images. No difference was found between values in terms of age, sex, cardiovascular risk factors, or drug use. The first row of values is shown in the examples retina and previous figures in this paper. The figure shows:

- Area veins and arteries.
- Diameter of veins and arteries (D).
- Veins P (VP) = number of veins around the papilla.
- Veins A (VA)= number of veins that cross the corona outlined with radius=2*Rp. Rp is the radio of the papilla.
- Veins B (VB)= number of veins that cross the corona outlined with radius=3*Rp.
- Same values for arteries. And the ratios leaving the region around the papilla and out of the disc (which could serve as a reference of bifurcations that has been, though not in the manner in which they branch).

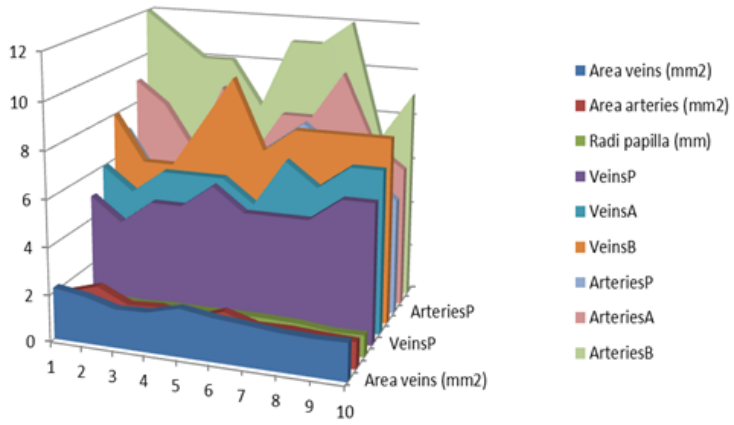

Fig. 7. Relations between the parameters obtained by the platform

It is possible to observe the measurement values of veins and arteries (thickness, area) are similar between different retinas (in this case not introduced any sick patient retinal image). Parameters like the veins in the papilla and AV index are the most fluctuating. Due to the lack of a common database and a reliable way to measure performance, it is difficult to compare our platform to those previously reported in the literature. Although some authors report algorithms and methods **¡Error! No se encuentra el origen de la referencia. ¡Error! No se encuentra el origen de la referencia. ¡Error! No se encuentra el origen de la referencia.¡Error! No se encuentra el origen de la referencia.¡Error! No se encuentra el origen de la referencia.¡Error! No se encuentra el origen de la referencia.** with similar performance than our platform, these results may not be comparable, since these methods are testing separately and were assessed using different databases.

3 Conclusions and Future work

This platform will show a high intra-observer and inter-observer reliability with the possibility of expert corrections if necessary. Results of its validity analysis must be consistent with the findings from large studies conducted with regards to both cardiovascular risk estimation and evaluation of target organ damage. The results obtained during the use of the platform will be connected and used to extract additional information by using reasoning models such as case-based reasoning (CBR) [4][18]. Platforms such as Altair offer the potential to examine a large number of images with time and cost savings and offer more objective measurements than current observer-driven techniques. Advantages in a clinical context include the potential to perform large numbers of automated screening for conditions such as risk of hypertension, left ventricular hypertrophy, metabolic syndrome, stroke, and coronary artery disease, which in turn reduces the workload required from medical staff. As a future line of study in this point, the next step would be to analyze the significance of the measurements obtained with regard to their meaning in a medical context. That is, to describe the relationship of the results obtained to the risk of cardiovascular disease estimated with the Framingham or similar scale and markers of cardiovascular target organ damage. The platform is intended as a unified tool to link all the methods needed to automate all processes of measurement on the retinas. It uses the latest computer techniques both statistical and medical.

.

4 References

[1]. Akita, K., Kuga. H. A computer method of understanding ocular fundus images. Pattern Recogn., 16 (1982), pp. 431–443

[2]. Chaudhuri, S., Chatterjee, S., Katz, N., Nelson, M., Goldbaum, M., 1989a. Automatic detection of the optic nerve in retinal images. In: Proceedings of the IEEE International Conference on Image Processing, vol. 1. Singapore, pp. 1–5.

[3]. Chen, B., C. Tosha, M.B. Gorin, S. Nusinowitz. Analysis of Autofluorescent retinal images and measurement of atrophic lesion growth in Stargardt disease. Experimental Eye Research, Volume 91, Issue 2, August 2010, Pages 143-152

[4]. De Paz J.F., Rodríguez S., Bajo J., Corchado J.M. CBR System for Diagnosis of Patient. Pags.: 807-812 pags. Editorial / Publisher: IEEE Computer Society Press. Proceedings of HIS 2008. ISBN: 978-0-7695-3326-1. 2009

[5]. García-Ortiz, José I. Recio-Rodríguez, Javier Parra-Sanchez, Luis J. González Elena, María C. Patino-Alonso, Cristina Agudo-Conde, Emiliano Rodríguez-Sánchez, Manuel A. Gómez-Marcos, on behalf of the Vaso-risk group- A new tool to assess retinal vessel caliber. Reliability and validity of measures and their relationship with cardiovascular risk. www.jhypertension.com. Volume 30 Number . April 2012

[6]. Goldbaum, M. Katz, N. , Nelson, M., Haff L.The discrimination of similarly colored objects in computer images of the ocular fundus. Invest. Ophthalmol. Vis. Sci., 31 (1990), pp. 617–623

[7]. Heneghan, C., J. Flynn, M. O'Keefe, M. Cahill. Characterization of changes in blood vessel and tortuosity in retinopathy of prematurity using image analysis. Med. Image Anal., 6 (2002), pp. 407–429

[8]. Heras, E., F. De la Prieta, V. Julian, S. Rodríguez, V. Botti, J. Bajo and J.M. Corchado. Agreetment technologies and their use in cloud computing environments. In: Progress in Artificial Intelligence. Volume 1. Number 4. (2012).

[9]. Hoover, A., Goldbaum, M. Locating the optic nerve in a retinal image using the fuzzy convergence of the blood vessels. IEEE Trans. Biomed. Eng., 22 (2003), pp. 951–958

[10]. Hoover, A., Kouznetsoza, V., Goldbaum, M. Locating blood vessels in retinal images by piecewise threshold probing of a matched filter response.IEEE Trans. Med. Imag., 19 (2000), pp. 203–210

[11]. Hunter, A., Lowell, J., Steel, D., Basu, A., Ryder, R., 2002. Non-linear filtering for vascular segmentation and detection of venous beading. University of Durham.

[12]. Jagoe Roger, J. Arnold, C. Blauth, P.L.C. Smith, K.M. Taylor, R. Wootton. Measurement of capillary dropout in retinal angiograms by computerised image analysis. Pattern Recognition Letters, Volume 13, Issue 2, February 1992, Pages 143-151.

[13]. Kalviainen, H., Hirvonen, P., Xu, L., Oja E. Probabilistic and non-probabilistic Hough transforms. Image Vision Comput., 13 (1995), pp. 239–252

[14]. Lee, S. ,Wang, Y., Lee E., A computer algorithm for automated detection and quantification of microaneurysms and haemorrhages in color retinal images.SPIE Conference on Image Perception and Performance, vol. 3663 (1999), pp. 61–71

[15]. Li,H., Chutatape, O. Automated feature extraction in color retinal images by a model based approach IEEE Trans. Biomed. Eng., 51 (2004), pp. 246–254

[16]. Lowell, J. A. Hunter, D. Steel, A. Basu, R. Ryder, L. Kennedy. Measurement of retinal vessel widths from fundus images based on 2-D modeling. IEEE Trans. Biomed. Eng., 23 (2004), pp. 1196–1204

[17]. Patton, Niall,Tariq M. Aslam, Thomas MacGillivray, Ian J. Deary, Baljean Dhillon, Robert H. Eikelboom, g, Kanagasingam Yogesan, Ian J. Constable (2006) Retinal image analysis: Concepts, applications and potential. Progress in Retinal and Eye Research.Elsevier.Volume 25, Issue 1, January 2006, Pages 99–127

[18]. Rodríguez S., De Paz J.F., Bajo J. and Corchado J.M. Applying CBR Sytems to Micro-Array Data Classification. Springer Velag. Advances in Soft Computing Series. Proceedings of IWPACBB 2008. ISBN: 978-3-540-85860-7. 2010

[19]. Sánchez, C., Hornero, R., López, M.I., Aboy, M., Poza, J., Abásolo, D. A novel automatic image processing algorithm for detection of hard exudates based on retinal image analysis. Medical Engineering & Physics, Volume 30, Issue 3, April 2008, Pages 350-357

[20]. Tamura, S., Okamoto, Y., Yanashima, K. Zero-crossing interval correction in tracing eye-fundus blood vessels Pattern Recogn., 21 (1988), pp. 227–233

[21]. Tanabe Y, Kawasaki R, Wang JJ, Wong TY, Mitchell P, Daimon M, et al. Retinal arteriolar narrowing predicts 5-year risk of hypertension in Japanese people: the Funagata study. Microcirculation 2010; 17:94–102.

[22]. Wong TY, Duncan BB, Golden SH, Klein R, Couper DJ, Klein BE, et al. Associations between the metabolic syndrome and retinal microvascular signs: the Atherosclerosis Risk In Communities study. Invest Ophthalmol Vis Sci 2004; 45:2949–2954.

[23]. Wong TY, Klein R, Sharrett AR, Duncan BB, Couper DJ, Tielsch JM, et al. Retinal arteriolar narrowing and risk of coronary heart disease in men and women. The Atherosclerosis Risk in Communities Study. JAMA 2002; 287:1153–1159.

[24]. Yatsuya H, Folsom AR, Wong TY, Klein R, Klein BE, Sharrett AR. Retinal microvascular abnormalities and risk of lacunar stroke: Atherosclerosis Risk in Communities Study. Stroke 2010; 41:1349–1355.